

A Game-Theoretic Framework for Coexistence of WiFi and Cellular Networks in the 6-GHz Unlicensed Spectrum

Aniq Ur Rahman¹, Mustafa A. Kishk², *Member, IEEE*, and Mohamed-Slim Alouini³, *Fellow, IEEE*

Abstract—The recently unlocked 6-GHz spectrum is accessible to cellular and WiFi networks for unlicensed use while they conform to the constraints imposed by the incumbent nodes. We allow only a fraction of the cellular base stations (BSs) and a fraction of WiFi access points (APs) to use the 6-GHz band so that sources of interference are spatially segregated and made sparse, thereby decreasing the overall interference to each other. Through our proposed framework, we control this fraction as we group portions of cellular and WiFi network elements into entities competing with the other entities for the spectrum resources. These entities interact to satisfy their Quality of Service demands by playing a non-cooperative game. The action of an entity corresponds to the fraction of its network elements (WiFi APs and cellular BSs) operating in the 6-GHz band. We use tools from stochastic geometry to derive the theoretical performance metrics for users of each radio access technology, which helps us capture the aggregate behaviour of the network in a snapshot. Due to the decentralized nature of the game, we find the solution using distributed Best Response Algorithm (D-BRA), which improves the average datarate by 11.37% and 18.59% for cellular and WiFi networks, respectively, with random strategy as the baseline. The results demonstrate how the system parameters affect the performance of a network at equilibrium and highlight the throughput gains of the networks as a result of using the 6-GHz bands, which offer considerably larger bandwidths. We tested our framework using real-world data, which shows that practical implementation of multi-entity spectrum sharing is feasible even when the spatial distribution of the network elements and population are non-homogeneous.

Index Terms—Spectrum sharing, game theory, stochastic geometry, distributed systems, 5G NR-U, Wi-Fi 6E.

I. INTRODUCTION

FEDERAL Communications Commission (FCC) has recently unlocked the 6 GHz band (from 5.925 GHz to

Manuscript received 2 February 2022; revised 28 July 2022 and 13 September 2022; accepted 4 October 2022. Date of publication 11 October 2022; date of current version 8 February 2023. The work is funded by the KAUST office of sponsored research. The associate editor coordinating the review of this article and approving it for publication was L. Wang. (Corresponding author: Aniq Ur Rahman.)

Aniq Ur Rahman was with the Department of Electrical and Computer Engineering, King Abdullah University of Science and Technology, Thuwal 23955, Saudi Arabia. He is now with the Department of Engineering Science, University of Oxford, OX1 2JD Oxford, U.K. (e-mail: aniq.rahman@eng.ox.ac.uk).

Mustafa A. Kishk is with the Department of Electronic Engineering, National University of Ireland, Maynooth, W23 F2H6 Ireland (e-mail: mustafa.kishk@mu.ie).

Mohamed-Slim Alouini is with the CEMSE Division, King Abdullah University of Science and Technology, Thuwal 23955, Saudi Arabia (e-mail: slim.alouini@kaust.edu.sa).

Digital Object Identifier 10.1109/TCCN.2022.3213732

7.125 GHz) for unlicensed users in U.S. [1], [2]. This *beachfront* 6-GHz spectrum has also been unlocked for unlicensed use in United Kingdom, Saudi Arabia, South Korea, Canada, Brazil and many countries in the European Union [3], [4], [5]. This unlicensed spectrum will be used by both WiFi users (Wi-Fi 6E) and cellular users (5G new radio unlicensed or NR-U) [6], [7], [8]. In addition, restriction will be applied on unlicensed users to ensure no interference is experienced by the incumbent nodes¹ [9], which includes fixed point communications such as wireless backhaul [10]. In order to study this new system setup, two types of coexistence needs to be taken into consideration: (i) the coexistence between the unlicensed users and the incumbent nodes, and (ii) the coexistence between WiFi and 5G users. For the former, as stated earlier, the restrictions deployed by standardization entities will govern the interplay between licensed and unlicensed users. However, such restrictions do not exist for the latter. In particular, WiFi and 5G users, while respecting the aforementioned restrictions, will both try to adjust their system parameters to maximize their Quality of Service (QoS), such as coverage or throughput.

Conventionally, the users prefer WiFi over cellular connection to access faster and more reliable Internet [11], but this behaviour is changing, as the cost of cellular Internet is decreasing, thereby incentivizing its use over WiFi [12]. Moreover cellular BSs cover a larger area compared to WiFi APs, which means that handovers are not that frequent, even for mobile users like vehicles and aerial drones. These differences in the use cases hint at the coexistence of these technologies instead of one taking over the other. The convergence between WiFi and 5G will open new business avenues and ultimately improve the user experience [13], as the two radio access technologies (RATs) will simultaneously complement each other while competing for the available bandwidth [12]. Therefore, improvement in the performance of both RATs is essential for transitioning into the future smoothly.

The proponents of the *Digital Inclusion* movement see spectrum sharing and unlicensed spectrum usage as potential solutions to make communication technologies affordable for rural and low-income neighborhoods [14], [15]. The

¹Incumbent nodes refer to the devices which are licensed to use the 6-GHz spectrum, such as BSs forming backhaul links, and emergency communication systems.

application of Listen-Before-Talk (LBT) schemes which work well for cognitive radios is not justified when the multiple networks are allowed to exploit the unlicensed spectrum without any preferential treatment. In LBT scheme, a secondary user transmits only when it senses that the channel interference level is below a threshold, to ensure that it is not being used by the primary user [16]. In the coexistence of WiFi and cellular networks in the 6-GHz bands, both of them are secondary users, so the LBT scheme cannot be enforced on either of the networks. This calls for an intelligent distributed algorithm which allocates the spectrum efficiently and minimizes the interference [14].

In this work, the network is divided among multiple entities [17], where each entity encompasses a portion of the WiFi and a portion of the cellular network. An entity can decide what fraction of its network elements, namely, the WiFi access points (APs) and cellular base stations (BSs), will operate in the unlicensed 6-GHz band. The variation in this fraction affects the performance of the entity's networks. Therefore, the choice of this fraction must be optimal. Moreover, the decision of one entity affects the performance of other entities. This implies that the entities will take a series of decisions, one after the other, and finally settle at a decision which is mutually optimal for all the entities. The interaction of these entities can be modelled as a non-cooperative multi-player game. The performance of the networks of an entity and their respective QoS requirements are used to define the payoff function of that entity.

Through this approach, we spatially segregate the network elements based on frequency usage, i.e., only a certain fraction of cellular BSs and a certain fraction of the WiFi APs use the 6-GHz spectrum to minimize the interference while still trying to maximize the QoS in terms of average data rate.

A. Related Works

1) *Coexistence in the Unlicensed Spectra*: Recent surveys [8], [11], have reviewed the coexistence of WiFi and cellular networks in the 6 GHz unlicensed bands, and provided an extensive list of relevant literature. Fair coexistence of LTE with WiFi has been studied for the 5 GHz band [18]. In [19], the authors define fairness in terms of datarate. Proportional fairness demonstrated in [20], allows each RAT to access the unlicensed channel for equal amount of time, which is better in contrast to the notion of fairness championed by 3GPP. Recently, coexistence of 5G NR with WiFi is also being investigated in the 60 GHz mmWave band [21], [22]. Bao et al. [23] realize the coexistence of WiFi and cellular networks in unlicensed bands by time-sharing and power-allocation.

2) *Stochastic Geometry for Studying Coexistence*: Authors in [24] make use of tools from stochastic geometry to study the coexistence of narrow band (NB) and ultra-wide band (UWB) wireless nodes. In [25], the authors analyse the performance of an LTE-WiFi network coexisting in the unlicensed 5 GHz band using stochastic geometry. Authors in [26] study the coexistence of WiFi and NR-U in the 6-GHz unlicensed bands and focus on uplink transmissions. The work makes

use of stochastic geometry and reports performance superior to CSMA/CA.

3) *Spectrum Sharing Using Game Theory*: Spectrum sharing is of key significance in alleviating mutual interference and it allows multiple users to utilize the spectrum in parallel [27]. The cognitive radio literature [28], [29], [30], [31], [32] treats the open spectrum sharing problem as a game, where the secondary users compete for the unlicensed spectrum. The users' actions include varying certain parameters such as transmission power, access duration and modulation technique. The payoff is generally modelled as a function of the experienced quality of service, such as throughput or latency. Bairagi et al. [33] adopt a game-theoretic framework to formulate the problem of unlicensed spectrum sharing among WiFi and LTE networks. First, coexistence is achieved through time-sharing between LTE and WiFi users by the Kalai-Smorodinsky bargaining solution. Next, the resources are allocated to LTE users by a Q-learning based algorithm. Authors in [34] formulate the problem of white space spectrum sharing among users as a social group utility maximization game where each user tries to maximize the utility of its social group. In [35], the authors solve the problem of spectrum coexistence between cellular and WiFi users through Nash Bargaining, and the resources secured by the cellular network is then allocated through a one-sided matching game. The payoff is maximized while ensuring that the QoS requirements of the WiFi and cellular users is satisfied. Authors in [36] incentivize the cellular users to be served over the unlicensed spectrum. The spectrum allocation is carried out through solving a Bayesian matching game.

B. Contributions

The major contributions of our work are as follows:

- The behaviour of WiFi and 5G cellular networks is studied, as they utilize the unlicensed 6 GHz spectrum in addition to their licensed/legacy spectra, while respecting the constraints imposed by the incumbent nodes. The interaction of multiple entities is formulated as a non-cooperative game and the payoff function of each entity is defined as a weighted sum of the datarates achieved by the RAT(s) it owns. The payoff is non-zero only when the datarate requirements of the RAT(s) are satisfied.
- We tested the proposed framework on real-world network of Glasgow, U.K. where the spatial distribution of population and the network elements are non-homogeneous. The results suggest that a practical implementation of our framework² is feasible to improve the coexistence of WiFi and cellular networks utilizing the 6-GHz unlicensed spectrum.

The rest of the paper is organized as follows. In Section II we describe the system model and then develop a mathematical understanding of the performance metrics in the next section, Section III. In Section IV we propose a game theoretic framework to study the problem, and show the results in Section V. In Section VI, we test our framework on a real-world network

²The simulation and analysis codes are available at [35].

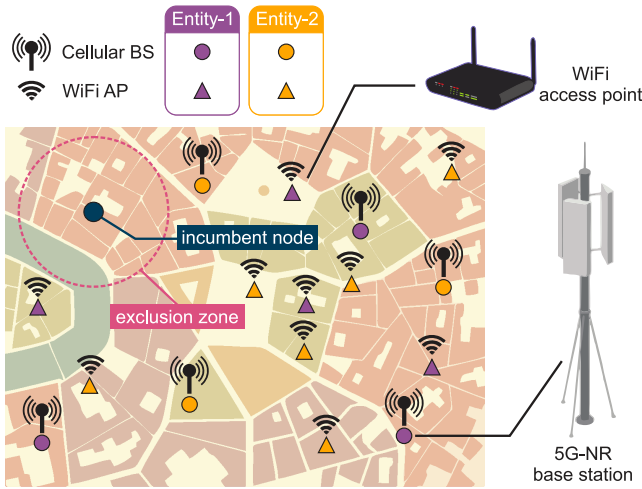


Fig. 1. System Illustration.

and assess the performance. The paper is finally concluded in Section VII.

II. SYSTEM MODEL

We consider a system where three coexisting wireless networks are utilizing the 6-GHz band: (i) the WiFi network consisting of the APs and the WiFi users, (ii) the cellular network consisting of cellular BSs and its users, and (iii) a network of the incumbent nodes, utilizing the 6-GHz band licensed to them for fixed point backhaul operation. We consider this to be the primary usage of this band and the performance of the first two networks should not hamper the experience of the incumbent nodes. To enforce this, each of these incumbent nodes have an *exclusion zone* around them, within which the 6-GHz band cannot be used by the WiFi and cellular networks [1], [2].

The WiFi APs and Cellular BSs are divided among various *entities*, i.e., parts of the network are owned by different mobile operators. The entities control their own utilization of the unlicensed spectrum to maximize their datarate in response to the 6-GHz spectrum utilization by the other entities. The interaction between the entities is modelled as a non-cooperative game. The system is illustrated in Fig. 1 and a sample network deployment scenario is presented in Fig. 2.

A. Network Deployment

1) *Incumbent Nodes*: We populate the \mathbb{R}^2 plane with incumbent nodes, which follow a homogeneous Poisson point process (PPP) Φ_z with parameter λ_z . Around each of these incumbent nodes, we have an exclusion zone of radius ρ . The set of all the exclusion zones is described mathematically as: $\Xi_\rho = \bigcup_{\mathbf{x} \in \Phi_z} b(\mathbf{x}, \rho)$, where $b(\mathbf{x}, \rho)$ denotes a disk of radius ρ centred at \mathbf{x} .

2) *WiFi Network*: Now we deploy the WiFi APs as a homogeneous PPP Φ_w of intensity λ_w . The set of APs which are allowed to use the unlicensed 6 GHz spectrum lie outside the exclusion zones Ξ_ρ and can be carved out as a Poisson Hole Process (PHP) from Φ_w . We define this PHP as

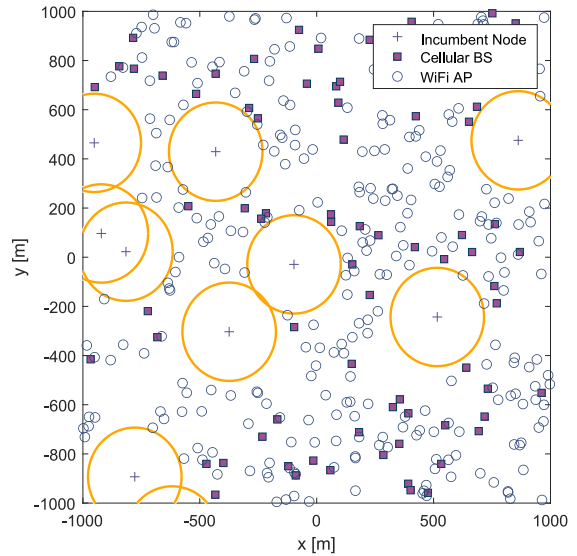


Fig. 2. Sample network deployment showing $\Phi_z, \Xi_\rho, \hat{\Phi}_c, \hat{\Phi}_w$. The exclusion zones of radius ρ are drawn around the incumbent nodes as yellow circles. Parameters: $\lambda_z = 1$ user/km², $\lambda_c = 25$ BS/km², $\lambda_w = 100$ AP/km², $\rho = 200$ m.

$\hat{\Phi}_w \triangleq \Phi_w \setminus \Xi_\rho$, which incorporates the effect of the exclusion zones in the system.

Approximation 1: The PHP $\hat{\Phi}_w$ can be approximated as a uniform PPP of intensity $\bar{\lambda}_w = \lambda_w \exp(-\pi\lambda_z\rho^2)$, see [36], [37].

A fraction $\delta_w \in [0, 1]$ of APs in $\hat{\Phi}_w$ operate in the unlicensed band. Therefore, we can write: $\Phi_w = \Phi_{w|L} \cup \Phi_{w|U}$, where $\Phi_{w|L}$ is the set of APs operating in their legacy 2.4GHz WiFi band, and $\Phi_{w|U}$ is set of APs using the unlicensed 6-GHz band. Furthermore, we can approximate $\Phi_{w|L}$ and $\Phi_{w|U}$ as independent homogeneous PPPs, such that: $\Phi_{w|U} \triangleq \text{PPP}(\delta_w \bar{\lambda}_w)$, and $\Phi_{w|L} \triangleq \text{PPP}(\lambda_w - \delta_w \bar{\lambda}_w)$, where $\text{PPP}(\Lambda)$ denotes a homogeneous Poisson point process having intensity Λ .

The WiFi users form a cluster point process, where each cluster has a radius ρ_w , and is centred around an AP. The WiFi users are denoted as Ψ_w and described as: $\Psi_w = \bigcup_{\mathbf{x} \in \Phi_w} \psi_{\mathbf{x}} + \mathbf{x}$, where $\psi_{\mathbf{x}}$ is a Matérn cluster centred around \mathbf{x} . In a Matérn cluster, the distance between a point in the cluster to the center follows a triangular distribution bounded within $(0, \rho_w)$, see [38].

3) *Cellular Network*: Similar to the deployment of the WiFi APs, we model the set of cellular BSs as an independent homogeneous PPP Φ_c of intensity λ_c , such that only the BSs lying outside the exclusion zones are permitted to utilize the unlicensed 6-GHz spectrum. The set of BSs outside the exclusion zones is a PHP $\hat{\Phi}_c = \Phi_c \setminus \Xi_\rho$ and a fraction $\delta_c \in [0, 1]$ of BSs in $\hat{\Phi}_c$ operate in the unlicensed band.

Approximation 2: The PHP $\hat{\Phi}_c$ is approximated as a homogeneous PPP with intensity $\bar{\lambda}_c = \lambda_c \exp(-\pi\lambda_z\rho^2)$, see [36], [37].

Alternatively, Φ_c can be described as: $\Phi_c = \Phi_{c|L} \cup \Phi_{c|U}$, where $\Phi_{c|L} \triangleq \text{PPP}(\lambda_c - \delta_c \bar{\lambda}_c)$ and $\Phi_{c|U} \triangleq \text{PPP}(\delta_c \bar{\lambda}_c)$ operate in the licensed and unlicensed bands, respectively.

Furthermore, the cellular users are spread in \mathbb{R}^2 as an independent homogeneous PPP.

The transmit powers of the cellular BSs, WiFi APs and incumbent nodes are p_c , p_w and p_z respectively. The bandwidth offered by the unlicensed 6-GHz band is B_U . The bandwidths of the cellular and WiFi networks operating in their corresponding licensed/legacy bands is denoted as $B_{c|L}$ and $B_{w|L}$, respectively. We also denote the bandwidths of the cellular and WiFi users in the unlicensed band as $B_{c|U}$ and $B_{w|U}$ respectively, and both are equal to B_U in value.

B. Downlink Interference

Definition 1: The user at the origin receives a signal of strength $\xi(\mathbf{x})$ from the transmitting node at \mathbf{x} : $\xi(\mathbf{x}) = p_x H \|\mathbf{x}\|^{-\alpha}$, where p_x is the transmit power of the node \mathbf{x} and $H \sim \exp(1)$ is the random variable signifying the channel gain due to Rayleigh fading and α is the path-loss coefficient.

In *unlicensed access*, the typical user experiences interference from all the networks utilizing the unlicensed 6-GHz spectrum, namely, Φ_z , $\Phi_{c|U}$ and $\Phi_{w|U}$. We define this set as $\Phi^U \triangleq \Phi_z \cup \Phi_{c|U} \cup \Phi_{w|U}$. The interference to cellular and WiFi users in unlicensed access is denoted as $I_{c|U}$ and $I_{w|U}$, respectively, and defined as follows:

$$I_{c|U} \triangleq \sum_{\mathbf{x} \in \Phi^U \setminus \{\mathbf{x}_0\}} \xi(\mathbf{x}), \quad \mathbf{x}_0 = \arg \min_{\mathbf{x} \in \Phi_{c|U}} \|\mathbf{x}\|, \quad (1)$$

$$I_{w|U} \triangleq \sum_{\mathbf{x} \in \Phi^U \setminus \{\mathbf{x}_0\}} \xi(\mathbf{x}), \quad \mathbf{x}_0 \sim \left\{ \mathbf{x} \in \Phi_{w|U} : \|\mathbf{x}\| < \rho_w \right\}. \quad (2)$$

In *licensed or legacy access*, the typical user experiences interference from its own network. The cellular and WiFi users receive interference from the nodes in $\Phi_{c|L}$ and $\Phi_{w|L}$ respectively. The interference to cellular and WiFi users in licensed/legacy access is denoted as $I_{c|L}$ and $I_{w|L}$ respectively, and defined as follows:

$$I_{c|L} \triangleq \sum_{\mathbf{x} \in \Phi_{c|L} \setminus \{\mathbf{x}_0\}} \xi(\mathbf{x}), \quad \mathbf{x}_0 = \arg \min_{\mathbf{x} \in \Phi_{c|L}} \|\mathbf{x}\|, \quad (3)$$

$$I_{w|L} \triangleq \sum_{\mathbf{x} \in \Phi_{w|L} \setminus \{\mathbf{x}_0\}} \xi(\mathbf{x}), \quad \mathbf{x}_0 \sim \left\{ \mathbf{x} \in \Phi_{w|L} : \|\mathbf{x}\| < \rho_w \right\}. \quad (4)$$

It must be noted that unlike the cellular users, the WiFi users do not connect to the nearest AP. Instead, they are connected to any single AP while being within its range. This is expressed mathematically in equations (2) and (4) as $\mathbf{x}_0 \sim \left\{ \mathbf{x} \in \Phi_{w|M} : \|\mathbf{x}\| < \rho_w \right\}$, $M \in \{U, L\}$, where \mathbf{x}_0 is the AP, to which the WiFi user connects. Next, we define the signal-to-interference-plus-noise ratio (SINR), which is ultimately used for the downlink analysis in the upcoming section.

Definition 2: The signal-to-interference-plus-noise ratio for a typical user is defined as: $\text{SINR}_{k|M} \triangleq \frac{\xi(\mathbf{x}_0)}{\kappa_k^2 + I_{k|M}}$; $k \in \{c, w\}$, $M \in \{U, L\}$, where κ_c^2 and κ_w^2 are the receiver noise power for the cellular and WiFi users respectively.

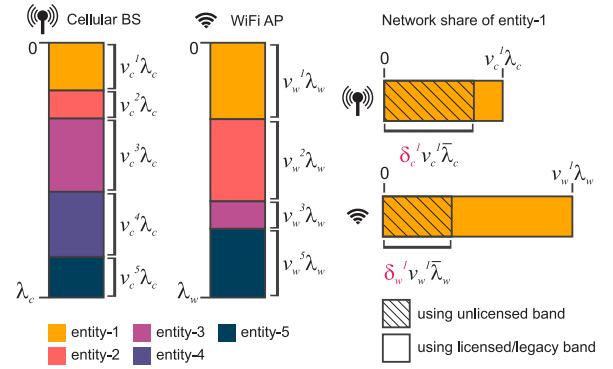


Fig. 3. Division of the network among a set of Entities.

C. Multi-Entity Competition

In simple words, an entity can be thought of as a Mobile Network Operator (MNO) which uses multiple WiFi APs and cellular BSs to provide service to its subscribers. It is seen in [17] that Mobile Virtual Network Operators (MVNOs) which are a conglomeration of multiple MNOs can generate more revenue compared to multiple MNOs operating independently. Therefore, we can envisage the entity being an MVNO having both RATs under its umbrella, which then allocates the resources judiciously in order to achieve the best overall performance. For example, Google has launched its own MVNO by the name of Google Fi [39] which aims at improving the QoS by smartly switching between WiFi and cellular networks.

We begin by defining a set of entities, $e_i \in \mathcal{E}$ which consists of a cellular network and a WiFi network. Entity e_i 's share of the cellular network is v_c^i and its share of WiFi network is v_w^i , such that, $\sum_{e_j \in \mathcal{E}} v_c^j = 1$, and $\sum_{e_j \in \mathcal{E}} v_w^j = 1$. The network of type $k \in \{c, w\}$ owned by entity e_i is denoted as $\Phi_k^i \triangleq \text{PPP}(v_k^i \lambda_k)$. The portion of Φ_k^i which lies outside the exclusion zones is denoted as $\hat{\Phi}_k^i \triangleq \text{PPP}(v_k^i \bar{\lambda}_k)$. A fraction δ_c^i of the cellular BSs $\in \hat{\Phi}_c^i$ and a fraction δ_w^i of the WiFi APs $\in \hat{\Phi}_w^i$ operate in the unlicensed 6-GHz band. The fraction of network elements in Φ_k^i which operate in the licensed/legacy and unlicensed bands are denoted as $\Phi_{k|L}^i \triangleq \text{PPP}(\delta_k^i v_k^i \bar{\lambda}_k)$, and $\Phi_{k|U}^i \triangleq \text{PPP}(v_k^i \lambda_k - \delta_k^i v_k^i \bar{\lambda}_k)$, respectively. Moreover, each entity has its own QoS requirement in the form of minimum datarates for its WiFi and cellular networks. The minimum datarate requirements of e_i for the cellular and WiFi networks are denoted as $\hat{\sigma}_c^i$ and $\hat{\sigma}_w^i$, respectively. The concept of entities is illustrated in Fig. 3. Finally, we present a formal definition for an entity as follows:

Definition 3: An entity $e_i \in \mathcal{E}$ can be defined by the tuple $(v_c^i, v_w^i, \delta_c^i, \delta_w^i, \hat{\sigma}_c^i, \hat{\sigma}_w^i)$, with the following description: (1) v_c^i is the cellular network share, (2) v_w^i is the WiFi network share, (3) δ_c^i is the cellular unlicensed spectrum utilization, (4) δ_w^i is the WiFi unlicensed spectrum utilization, (5) $\hat{\sigma}_c^i$ is the cellular datarate threshold, (6) $\hat{\sigma}_w^i$ is the WiFi datarate threshold.

In this model, $v_c^i = 0$ implies that the entity lacks a cellular network and $v_w^i = 0$ denotes the absence of a WiFi network. In the context of the entire network, the fraction denoting the utilization of the unlicensed band by the cellular

and WiFi networks is defined as $\delta_c \triangleq \sum_{e_j \in \mathcal{E}} v_c^j \delta_c^j$ and $\delta_w \triangleq \sum_{e_j \in \mathcal{E}} v_w^j \delta_w^j$ respectively.

III. PERFORMANCE METRICS

In this section we derive the performance metrics, which are used to define the payoff function in the game-theoretic formulations in the next section.

A. Coverage Probability

We begin by presenting the theoretical expressions of coverage probability for the cellular and WiFi networks operating in the different bands based on the parameters discussed in Section II. Formally, we define the coverage probability as follows:

Definition 4: Coverage Probability is defined as the probability that the SINR experienced by a user is greater than the threshold value of γ , i.e., $P_{k|M} \triangleq \mathbb{P}(\text{SINR}_{k|M} > \gamma)$, where $k \in \{c, w\}$ denotes the network (cellular/WiFi), and $M \in \{U, L\}$ denotes the mode of access (U for unlicensed and L for licensed/legacy).

1) *Cellular Users:* The coverage probability for cellular users operating in the licensed and unlicensed bands are described in Lemma 1 and Lemma 2 respectively, as follows.

Lemma 1: The coverage probability for a cellular user operating in the licensed band is:

$$P_{c|L}(\gamma, \delta_c) = 2\pi(\lambda_c - \delta_c \bar{\lambda}_c) \int_0^\infty \exp\left\{-\frac{\kappa_c^2 \gamma}{p_c} r^\alpha - \pi(\lambda_c - \delta_c \bar{\lambda}_c)(1 + \zeta(\gamma, \alpha))r^2\right\} r dr, \quad (5)$$

where $\zeta(\gamma, \alpha) = \frac{\gamma^{\frac{2}{\alpha}}}{2} \int_{\gamma^{-\frac{2}{\alpha}}}^\infty \frac{1}{1+x^{\frac{\alpha}{2}}} dx$.

Proof: The proof is provided in [40, Proposition 5.2.3] and is hence skipped. ■

Lemma 2: The coverage probability for a cellular user in the 6-GHz unlicensed band is:

$$P_{c|U}(\gamma, \delta_c, \delta_w) = 2\pi\delta_c \bar{\lambda}_c \int_0^\infty \exp\left\{-\frac{\kappa_c^2 \gamma}{p_c} r^\alpha - \left(\frac{\pi\gamma^{2/\alpha}}{p_c^{2/\alpha} \text{sinc}(\frac{2}{\alpha})} \left(\delta_w \bar{\lambda}_w p_w^{\frac{2}{\alpha}} + \lambda_z p_z^{\frac{2}{\alpha}}\right) + \pi\delta_c \bar{\lambda}_c(1 + \zeta(\gamma, \alpha))\right)r^2\right\} r dr; \quad (6)$$

where $\zeta(\gamma, \alpha) = \frac{\gamma^{\frac{2}{\alpha}}}{2} \int_{\gamma^{-\frac{2}{\alpha}}}^\infty \frac{1}{1+x^{\frac{\alpha}{2}}} dx$.

Proof: Using the definition of SINR and coverage probability above, we express the coverage probability for a cellular user operating in the unlicensed band as: $P_{c|U}(\gamma, \delta_c, \delta_w) = \mathbb{P}\left(\frac{p_c H R^{-\alpha}}{\kappa_c^2 + I_{c|U}} > \gamma\right)$. Then we take the expectation over the two random quantities: the distance between the cellular user and its BS R , and the interference $I_{c|U}$. The distance R follows the distribution: $f_R^c(r) = 2\pi\delta_c \bar{\lambda}_c r \exp(-\pi\delta_c \bar{\lambda}_c r^2)$, $r \geq 0$. Further, exploiting the cumulative distribution function (CDF) of H which is exponentially distributed as $H \sim \exp(1)$, we

arrive at:

$$P_{c|U} = \int_0^\infty e^{-\kappa_c^2 p_c^{-1} \gamma r^\alpha} \prod_{j \in \{w, z, c\}} \mathcal{L}_{c,j|U}\left(\frac{r^\alpha \gamma}{p_c}\right) \times f_R^c(r) dr,$$

where $\mathcal{L}_{c,j|U}(s)$ is the Laplace transform of the interference experienced by the cellular users in the unlicensed band from transmitters of type $j \in \{c, w, z\}$. Plugging the expression for the Laplace transforms from the Appendix yields the final equation in the lemma. ■

2) *WiFi Users:* The coverage probability for WiFi users operating in the legacy and unlicensed bands are described in Lemma 3 and Lemma 4 respectively, as follows.

Lemma 3: The coverage probability for a WiFi user operating in the legacy WiFi band is:

$$P_{w|L}(\gamma, \delta_w) = \frac{2}{\rho_w^2} \int_0^{\rho_w} \exp\left\{-\frac{\kappa_w^2 \gamma}{p_w} r^\alpha - \frac{\pi\gamma^{2/\alpha}(\lambda_w - \delta_w \bar{\lambda}_w)}{\text{sinc}(\frac{2}{\alpha})} r^2\right\} r dr. \quad (7)$$

Proof: The proof is provided in [40, Proposition 5.2.1] and is hence skipped. ■

Lemma 4: The coverage probability for a WiFi user operating in the 6-GHz unlicensed band is:

$$P_{w|U}(\gamma, \delta_c, \delta_w) = \frac{2}{\rho_w^2} \int_0^{\rho_w} \exp\left\{-\frac{\kappa_w^2 \gamma}{p_w} r^\alpha - \frac{\pi\gamma^{2/\alpha}}{p_w^{2/\alpha} \text{sinc}(\frac{2}{\alpha})} \left(\delta_w \bar{\lambda}_w p_w^{\frac{2}{\alpha}} + \delta_c \bar{\lambda}_c p_c^{\frac{2}{\alpha}} + \lambda_z p_z^{\frac{2}{\alpha}}\right) r^2\right\} r dr. \quad (8)$$

Proof: The proof can be sketched on the same lines as shown in the proof of Lemma 2. Here, the distance R between a WiFi user and the AP it is associated with, follows the distribution: $f_R^w(r) = \frac{2r}{\rho_w^2} \cdot 1\{0 \leq r < \rho_w\}$. ■

In Fig. 4, we see that our theoretical expressions for coverage probability described in Lemmas 1-4, are in agreement with the Monte Carlo simulation results.

B. Average Datarate

In this section, we define the average datarate of typical cellular and WiFi users. Formally, it is defined as the average of the datarates experienced by the users associated with the network elements of an entity, either cellular or WiFi. In the following two theorems, we present theoretical expressions for the average datarate of the cellular and WiFi users, derived using Stochastic Geometry.

Theorem 1: The average datarate of a user served by the cellular network of entity e_i is:

$$\begin{aligned} \sigma_c^i(\gamma, \delta_c, \delta_w, \delta_c^i) &= B_{c|U} \log_2(1 + \gamma) P_{c|U}(\gamma, \delta_c, \delta_w) \cdot \frac{\delta_c^i \bar{\lambda}_c}{\lambda_c} \\ &\quad + B_{c|L} \log_2(1 + \gamma) P_{c|L}(\gamma, \delta_c) \\ &\quad \cdot \left(1 - \frac{\delta_c^i \bar{\lambda}_c}{\lambda_c}\right). \end{aligned} \quad (9)$$

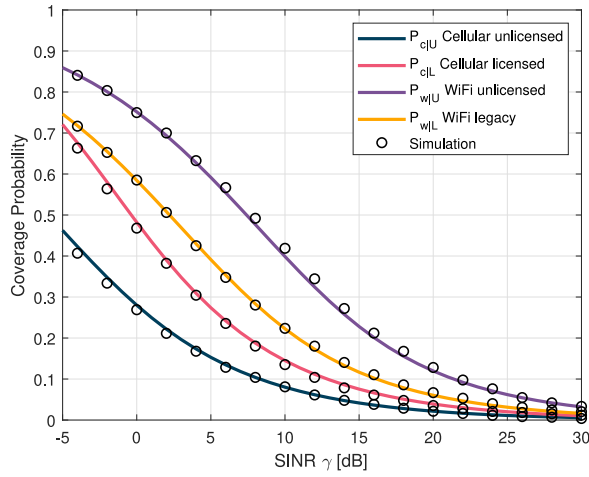


Fig. 4. Coverage probability for the cellular and WiFi users operating in the licensed and unlicensed spectra. $\lambda_z = 1$ user/km², $\lambda_c = 25$ BS/km², $\lambda_w = 100$ AP/km², $\rho = 200$ m, $\rho_w = 50$ m, $p_z = 1$ W, $p_c = 2$ W, $p_w = 1$ W, $\delta_c = 0.7$, $\delta_w = 0.2$.

Proof: We can express the time-averaged datarate of a cellular user associated with a BS $\mathbf{x} \in \Phi_c^i$ of entity e_i as: $B_x \log_2(1 + \gamma) \mathbb{P}(\text{SINR}_x > \gamma)$, where B_x is the bandwidth offered by \mathbf{x} . Taking expectation over Φ_c^i , we get:

$$\begin{aligned} \sigma_c^i &\stackrel{(a)}{=} \sum_{M \in \{U, L\}} \mathbb{E}_{\Phi_{c|M}^i} [B_x \log_2(1 + \gamma) \mathbb{P}(\text{SINR}_x > \gamma)] \\ &\stackrel{(b)}{=} \sum_{M \in \{U, L\}} \frac{|\Phi_{c|M}^i|}{|\Phi_c^i|} B_{c|M} \log_2(1 + \gamma) P_{c|M} \end{aligned}$$

Step (a) follows from $\Phi_c^i = \Phi_{c|U}^i \cup \Phi_{c|L}^i$. In step (b), $|\Phi|$ denotes the intensity of a PPP Φ . ■

Theorem 2: The average datarate of a user served by the WiFi network of entity e_i is:

$$\begin{aligned} \sigma_w^i(\gamma, \delta_c, \delta_w, \delta_w^i) &= B_{w|U} \log_2(1 + \gamma) P_{w|U}(\gamma, \delta_c, \delta_w) \cdot \frac{\delta_w^i \bar{\lambda}_w}{\lambda_w} \\ &\quad + B_{w|L} \log_2(1 + \gamma) P_{w|L}(\gamma, \delta_w) \\ &\quad \cdot \left(1 - \frac{\delta_w^i \bar{\lambda}_w}{\lambda_w}\right). \end{aligned} \quad (10)$$

Proof: The proof can be sketched on the same lines as Theorem 1, and is hence skipped. ■

In Fig. 5, we present the average cellular and WiFi datarates for various values of δ_c and δ_w . Changes in δ_c and δ_w essentially mean that the number of cellular and WiFi users operating in the 6-GHz band is changing respectively. The cellular datarate peaks at $\delta_c = 1$ and $\delta_w = 0$ implying that it performs the best in the absence of interference from the WiFi network in the unlicensed band. Moreover, for any value of δ_w , the maximum cellular datarate is observed at $\delta_c = 1$. However, the WiFi datarate has a maximum at $\delta_w \approx 0.7$ for any value of δ_c indicating that it performs best when the self-interference in the unlicensed band by the WiFi network is kept under check. In other words, if all the WiFi APs operate in the unlicensed band, the interference increases and aggravates the datarate. This suggests that the WiFi networks should under-utilize the 6-GHz spectrum for best results. These trends indicate a non-linear relationship between WiFi and cellular

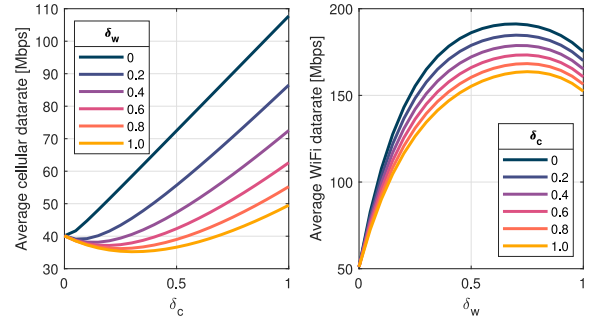


Fig. 5. Average cellular and WiFi datarates. Parameters: $|\mathcal{E}| = 1$, $\lambda_z = 1$ user/km², $\lambda_c = 25$ BS/km², $\lambda_w = 100$ AP/km², $\rho = 200$ m, $\rho_w = 50$ m, $p_z = 1$ W, $p_c = 2$ W, $p_w = 1$ W, $B_U = 240$ MHz, $B_{c|L} = 80$ MHz, $B_{w|L} = 80$ MHz, $\gamma = 10$ dB.

datarates based on the variation in 6-GHz spectrum utilization (δ_c, δ_w) by the entities. Therefore a dynamic policy is required which can settle at the optimal δ_c, δ_w values as the environment evolves.

In the next section, we invoke the concept of non-cooperative games to model the interaction between different entities, where each entity tries to maximize the value of its payoff function by taking the necessary action.

IV. GAME FORMULATION

Each entity e_i adjusts its unlicensed spectrum utilization δ_c^i, δ_w^i to maximize its own payoff function. The interaction of all the entities can be modelled as a non-cooperative game. Therefore we represent the action of entity e_i as a vector \mathbf{a}_i of unlicensed spectrum utilization factors as: $\mathbf{a}_i \triangleq [\delta_c^i, \delta_w^i]^T \in \mathcal{C}_\mu^2$, where $\mathcal{C}_\mu = \{0, \mu, 2\mu, \dots, 1\}$ is the discretized version of $[0, 1]$ with a step-size of μ to make the action space finite, thereby making the game finite. The set of actions of all the entities except e_i is denoted as: $\mathcal{A}_{-i} \triangleq \{\mathbf{a}_j : \forall e_j \in \mathcal{E} \setminus \{e_i\}\}$.

Definition 5: The payoff function of entity e_i is defined as $f_i(\mathbf{a}_i, \mathcal{A}_{-i}) : \mathcal{C}_\mu^{2|\mathcal{E}|} \mapsto \mathbb{R}$, which maps the actions of all the entities to a real value.

Definition 6: The game is defined as $\mathfrak{G}(\mathcal{E}, \mathcal{A}, \mathcal{F})$, where entities \mathcal{E} are the players, $\mathcal{A} \triangleq \mathcal{C}_\mu^{2|\mathcal{E}|}$ is the action profile and $\mathcal{F} \triangleq (f_i, \dots, f_{|\mathcal{E}|})$ is the set of payoff functions of all players.

In this non-cooperative framework, we impose a strict condition that the entities are not aware of the actions of other entities. When an entity takes an action, it is based on the observations from the environment and the action then alters the environment. Each network element of an entity can measure the power of the interfering signals in the licensed and unlicensed bands, and leverage this information to estimate the average datarate experienced by the users in its proximity.

Since there is no coordination among the entities, we cannot schedule the decision making process as a round-robin sequence. Instead we equip each entity with an independent Poisson clock [41] with the same rate, which triggers the entity to take an action (see Fig. 6). We also assume that the time taken by each entity to choose an action is small enough to make the probability of multiple entities acting simultaneously negligible.

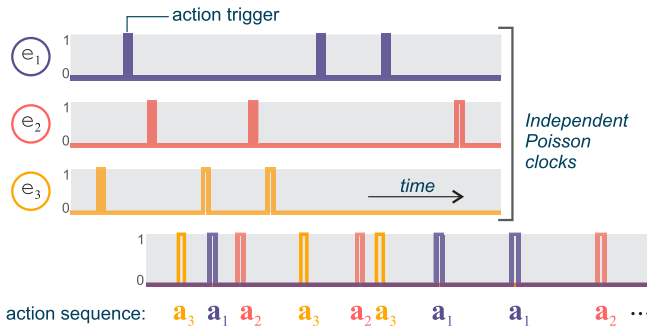


Fig. 6. Action sequence as a result of independent Poisson clocks.

Remark 1: The action sequence generated as a consequence of each entity being triggered by its Poisson clock is a sequence where each element is the action of an entity drawn from the set of all entities with uniform probability.

A. Payoff Function

We want to define the payoff function which the entities can adopt to find their best response. The aim of each entity is to maximize the weighted sum of the datarates of its networks while satisfying the demands of each network. This is framed as the following optimization problem:

$$\begin{aligned} \mathbf{P1}: \max_{\delta_c^i, \delta_w^i} & \theta_c^i \sigma_c^i + \theta_w^i \sigma_w^i \\ \text{s.t.} & \sigma_c^i \geq \hat{\sigma}_c^i, \sigma_w^i \geq \hat{\sigma}_w^i. \end{aligned}$$

The payoff function which encapsulates problem **P1** with its objective and constraints bound together as a single function is defined as:

$$f_i \triangleq 1_{\sigma_i} \times \sum_{k \in \{c, w\}} \theta_k^i \sigma_k^i 1\{v_k^i > 0\}, \quad (11)$$

where the condition that the cellular and WiFi datarates are greater than the minimum values, is indicated as $1_{\sigma_i} \triangleq 1\{\bigcap_{k \in \{c, w\}} (\sigma_k^i \geq \hat{\sigma}_k^i | v_k^i > 0)\}$. This ensures that the action which fulfils the minimum datarate will always be chosen in the presence of actions which might have a higher weighted sum of datarates but do not meet the datarate requirements for both networks simultaneously.

The *preference* for the cellular and WiFi networks in an entity e_i is translated by the weights $\theta_c^i > 0$ and $\theta_w^i > 0$ respectively, which are used in the definition of the payoff function below.

The concept of network preference terms θ_c and θ_w is introduced to balance the datarates of the WiFi and cellular networks and promote fair coexistence. The value of these weights can be set by the respective entity based on their own analysis. The effect of θ_c and θ_w is further explained in the results section (Section V-A).

B. Distributed Algorithm

We focus on finding the set of actions $[\mathbf{a}_1 \cdots \mathbf{a}_k \cdots \mathbf{a}_{|\mathcal{E}|}]$ which the entities collectively do not change in their subsequent iterations.

Algorithm 1 Distributed Best Response Algorithm (D-BRA)

```

1:  $\mathbf{a}_j \sim \mathcal{C}_\mu^2; \forall e_j \in \mathcal{E}$  ▷ Initialization
2:  $n_j \leftarrow 0; \forall e_j \in \mathcal{E}$ 
3: while  $\sum_{e_j \in \mathcal{E}} \|\mathbf{a}_j^{[n_j]} - \mathbf{a}_j^{[n_j-1]}\| > 0$  do
4:    $i \sim \text{uniform}(1, |\mathcal{E}|)$  ▷ Remark 1
5:    $\mathbf{a}_i \leftarrow \arg \max_{\mathbf{a} \in \mathcal{C}_\mu^2} f_i(\mathbf{a} | \mathcal{A}_{-i})$  ▷ Best Response: solved
     through exhaustive search in  $\mathcal{C}_\mu^2$ 
6:    $n_i \leftarrow n_i + 1$ 
7:    $\mathbf{A}_i^{[n_i]} \leftarrow \mathbf{a}_i$  ▷ Update action vector
8: end while
    
```

Definition 7: The solution of \mathfrak{G} is defined as the matrix of action vectors of all the entities $[\mathbf{a}_1^{[n_1]} \cdots \mathbf{a}_k^{[n_k]} \cdots \mathbf{a}_{|\mathcal{E}|}^{[n_{|\mathcal{E}|}]}]$ such that the action vector of each entity remains unchanged in their latest iterations, i.e., $\sum_{e_j \in \mathcal{E}} \|\mathbf{a}_j^{[n_j]} - \mathbf{a}_j^{[n_j-1]}\| = 0$, where

$\mathbf{a}_j^{[m]}$ denotes the action vector of e_j at the m^{th} iteration and n_j is the latest iteration of entity e_j .

The solution is equivalent to the Nash equilibrium, as the only reason why the players stop changing their action vectors collectively is because they have reached an ‘equilibrium’. Since the payoff functions are not straightforward, we avoid finding the solution analytically and therefore resort to the distributed best response algorithm (D-BRA) which is presented in Algorithm 1. The algorithm can be set to run at periodic intervals. This makes the system adaptive to environmental changes due to the addition or removal of nodes, or the introduction of rogue elements which perturb the equilibrium from time to time.

In step 5 of Algorithm 1, to find the value of $f_i(\mathbf{a} | \mathcal{A}_{-i})$ given the action of other entities \mathcal{A}_{-i} is fixed, we only need to supply one input, i.e., \mathbf{a} . Through exhaustive search, we can find a maximizer in the discrete search space \mathcal{C}_μ^2 .

Remark 2: When the game \mathfrak{G} does not have a *pure strategy* Nash equilibrium, D-BRA does not terminate. In such cases, if we analyze the action vectors of all the agents over a large number of iterations, the probability mass function of the action space \mathcal{A} converges in distribution³ to the *mixed strategy* Nash equilibrium, which is guaranteed to exist by the Folk theorem [43], [44], [45], [46], since \mathfrak{G} can be viewed as a repeated game in normal-form.

In practice, we can have $\sum_{e_j \in \mathcal{E}} \|\mathbf{a}_j^{[n_j]} - \mathbf{a}_j^{[n_j-1]}\| \leq \varepsilon$, where $\varepsilon > 0$ is an arbitrarily small value which controls the accuracy of the solution. This way, we get an approximate solution in the ε -neighborhood of the exact solution which can make the algorithm converge faster, albeit to a near-optimal solution. To improve the accuracy of the solution further, we can reduce the value of the step-size μ to refine the search space. Intuitively, the complexity of D-BRA increases with increase in number of entities $|\mathcal{E}|$ and search space size $|\mathcal{C}_\mu|$ but the exact characterization deserves a thorough mathematical investigation and is therefore beyond the scope of this work.

³Supported by [42, Proposition 2.2].

TABLE I
RANGE OF SYSTEM PARAMETERS

Parameter	Values	Source
B_U	$\in [40, 80, 160, 240, 320]$ MHz	[8], [11]
$B_{c L}$	$\in [20, 40, 80, 100]$ MHz	[47]
$B_{w L}$	$\in [20, 40, 80, 160]$ MHz	[48]
p_z	≤ 30 dBm	[8]
p_c	≤ 36 dBm	[8]
p_w	≤ 36 dBm	[8]
λ_z	1 km^{-2}	[49]
λ_c	$\in [25, 50, 250] \text{ km}^{-2}$	[50], [51]
λ_w	$\in [100, 400] \text{ km}^{-2}$	[52]
ρ	200 m	
ρ_w	50 m	[53]

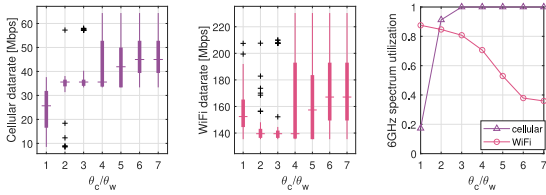


Fig. 7. Average cellular and WiFi datarates at Equilibrium for different values of θ_c/θ_w . $|\mathcal{E}| = 2$, $\hat{\sigma}_c = 30$ Mbps, $\hat{\sigma}_w = 100$ Mbps, $\gamma = 10$ dB.

V. RESULTS & DISCUSSION

We present the results for the interaction between the entities and analyse how the various parameters affect the datarate achieved by the entities at equilibrium, in order to provide useful design insights for implementation. The range of the parameters used in the system model are summarized in Table I. For all the results that follow, we use the following values: $\lambda_z = 1$ user/km², $\lambda_c = 25$ BS/km², $\lambda_w = 100$ AP/km², $\rho = 200$ m, $\rho_w = 50$ m, $p_z = 1$ W, $p_c = 2$ W, $p_w = 1$ W, $B_U = 240$ MHz, $B_{c|L} = 80$ MHz, $B_{w|L} = 80$ MHz, $\gamma = 10$ dB, $\mu = 0.1$.

A. Effect of Network Preference

We define two entities, each demanding a minimum cellular datarate of 30 Mbps and minimum WiFi datarate of 100 Mbps. To visualize the behaviour of the payoff function, we vary the ratio θ_c^i/θ_w^i and plot the values of cellular and WiFi datarates summarized for $(v_c^i, v_w^i) \in [0.1, 0.9]^2$. In Fig. 7, the mean value of the average cellular datarate increases with an increase in the ratio. This implies that as the entity gives more preference to its cellular network, its performance improves. An interesting trend is observed for the WiFi datarates. After a dip at $\theta_c = 2\theta_w$, it rises back up $\theta_c = 5\theta_w$ onwards. This can be explained by looking at how the 6-GHz spectrum is utilized for $\theta_c/\theta_w = 1$ case. Here the cellular networks rely mostly on their licensed band, which reduces interference to the WiFi networks operating in the 6-GHz unlicensed bands, thereby increasing their datarate, as observed.

In Fig. 8, for the same entities playing the same game, the Nash equilibrium changes due to difference in the value of the ratio θ_c/θ_w . In Fig. 8(a), we give 7 times more preference to the cellular network datarate compared to its WiFi counterpart, due to which the cellular datarate of both entities settle

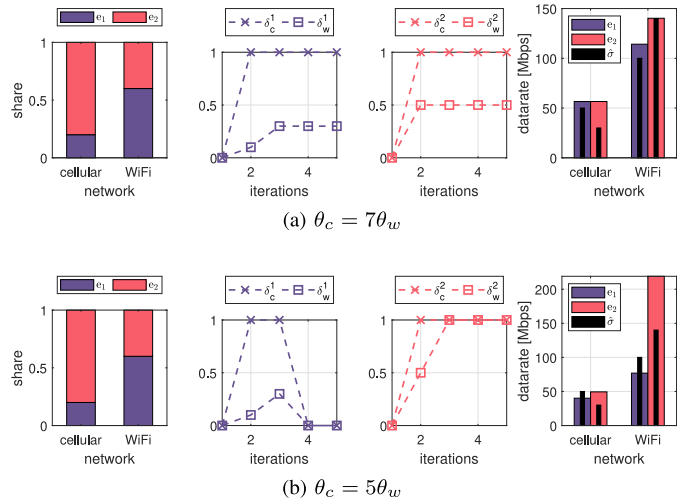


Fig. 8. Nash Equilibria due to difference in θ_c/θ_w . $|\mathcal{E}| = 2$.

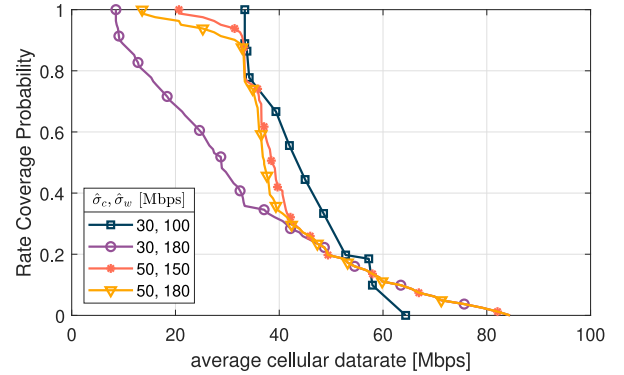


Fig. 9. Empirical CCDF of average cellular datarate. Parameters: $|\mathcal{E}| = 2$, $\theta_c/\theta_w = 7$.

at ~ 55 Mbps which satisfies the datarate requirement of both the entities. Moreover, the equilibrium is satisfactory for both networks of each entity. In contrast, in Fig. 8(b) where $\theta_c = 5\theta_w$ we observe that the datarate requirements of entity-1 are not met at all. This could be attributed to entity-2 greedily setting δ_w^2 value to 1 to maximize its WiFi datarate. In the subsequent iterations, none of the actions by entity-1 could satisfy its datarates, so it saturates at $\delta_c^1 = 0, \delta_w^1 = 0$. Therefore tuning the value of the ratio θ_c/θ_w is essential for system performance.

B. Effect of Datarate Thresholds

We study two entities with identical datarate requirements and vary $(v_c^1, v_w^1) \in [0.1, 0.9]^2$. Then, we analyse the empirical *complementary cumulative density function* (CCDF) of the cellular and WiFi datarates for different values of minimum cellular and WiFi datarate thresholds. The value of this CCDF at x , is referred to as the *rate coverage probability* (RCP) at datarate threshold equal to x .

We first comment on the variation in average cellular datarate due to different datarate thresholds as shown in Fig. 9 and we observe the following:

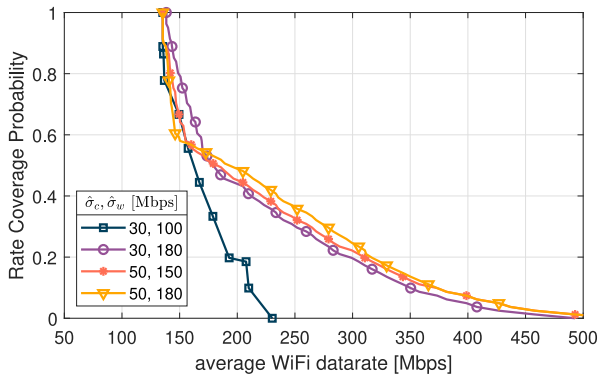


Fig. 10. Empirical CCDF of average WiFi datarate. Parameters: $|\mathcal{E}| = 2$, $\theta_c/\theta_w = 7$.

- The datarate requirement is perfectly met when the WiFi datarate threshold $\hat{\sigma}_w$ is low (100 Mbps) as well as the cellular datarate threshold $\hat{\sigma}_c$ is low (30 Mbps).
- Setting the cellular datarate threshold to a value higher than the true requirement ensures a higher rate coverage probability (RCP) at the true requirement. For example, when $\hat{\sigma}_c = 50$ Mbps and $\hat{\sigma}_w = 180$ Mbps, the RCP at 50 Mbps is ~ 0.2 , but it shoots up to ~ 0.9 at 30 Mbps.
- The RCP decreases with increase in the WiFi datarate threshold $\hat{\sigma}_w$.

Next, we comment on the variation in the average WiFi datarate due to datarate thresholds. The rate coverage probability of average WiFi datarate is presented in Fig. 10, based on which we make the following observations:

- The rate coverage probability is 1 when the WiFi datarate threshold is low, i.e., $\hat{\sigma}_w = 100$ Mbps.
- For the same cellular datarate threshold $\hat{\sigma}_c$, the RCP increases on increasing the WiFi datarate threshold $\hat{\sigma}_w$.
- The RCP decreases as the cellular datarate threshold $\hat{\sigma}_c$ is increased.

C. Datarate Improvements

Here, we compare the performance of our algorithm D-BRA with a random strategy, where the values of δ_c and δ_w are randomly chosen from the closed set $[0.1, 1]$. We call this strategy RANDOM. In Fig. 11, we clearly see that D-BRA outperforms RANDOM. Moreover, comparing the mean values of the average datarates, we find that D-BRA improves the performance of cellular networks by 11.37% and of WiFi networks by 18.59%.

D. Cellular vs. WiFi

We consider a special case, where one entity owns the cellular network entirely and the other entity owns the complete WiFi network. In Fig. 12, the datarate requirements of both entities are satisfied at equilibrium. The cellular network in both cases, settles at $\delta_c^1 = 1$, while the WiFi network settles at $\delta_w^2 \approx 0.4$ when $\hat{\sigma}_w^2 = 120$ Mbps in Fig. 12(a) and at $\delta_w^2 \approx 0.5$ when $\hat{\sigma}_w^2 = 130$ Mbps in Fig. 12(b). Due to the increase in WiFi datarate threshold, the cellular datarate decreases in Fig. 12(b), even though the minimum cellular datarate requirement is still met.

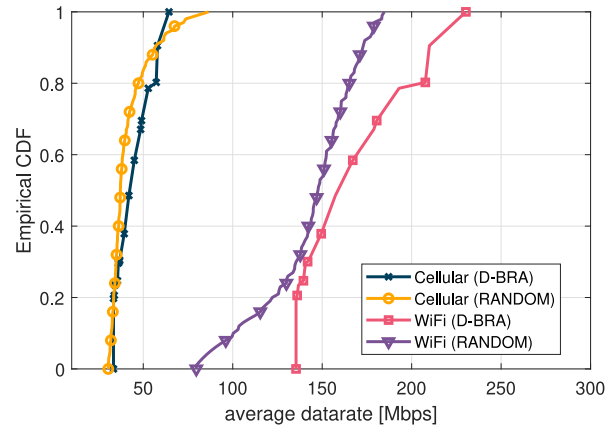


Fig. 11. Empirical CDF of the average datarates. Parameters: $\theta_c/\theta_w \in \{5, 6, 7\}$, $|\mathcal{E}| = 2$, $\hat{\sigma}_c = 30$ Mbps, $\hat{\sigma}_w = 100$ Mbps, $\gamma = 10$ dB.

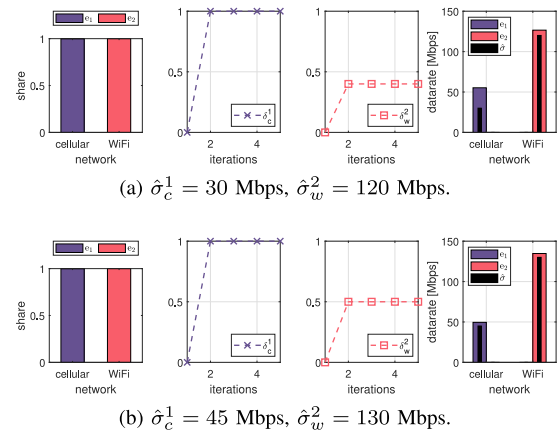


Fig. 12. Interaction of two entities when one entity is entirely cellular and the other is entirely WiFi: $v_c^1 = 1$, $v_w^2 = 1$. Parameters: $|\mathcal{E}| = 2$, $\theta_c = 7\theta_w$.

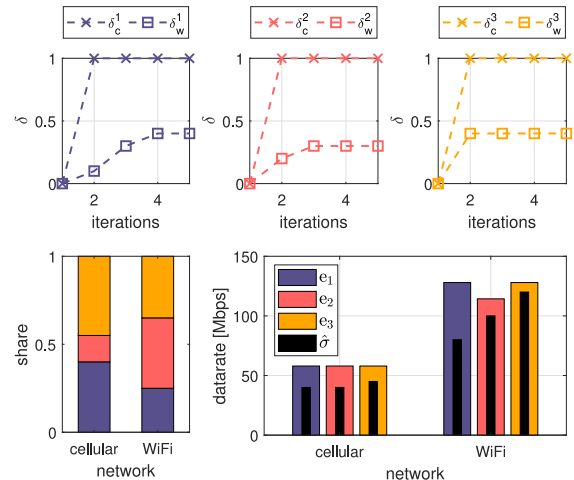


Fig. 13. Exemplary three-entity interaction, $\theta_c = 7\theta_w$.

E. Three-Entity Game

Next, we demonstrate that our framework works for more than two entities.⁴ Here three entities owning different shares

⁴Currently, most countries have 3-4 major Telecom companies. For example, U.S. has AT&T, Verizon and T-Mobile among the major players. Similarly, India has Reliance Jio, Airtel and Vodafone-Idea. Therefore, in our simulations, when we show the interaction of 2 entities and 3 entities, it very well captures the existing scenario.

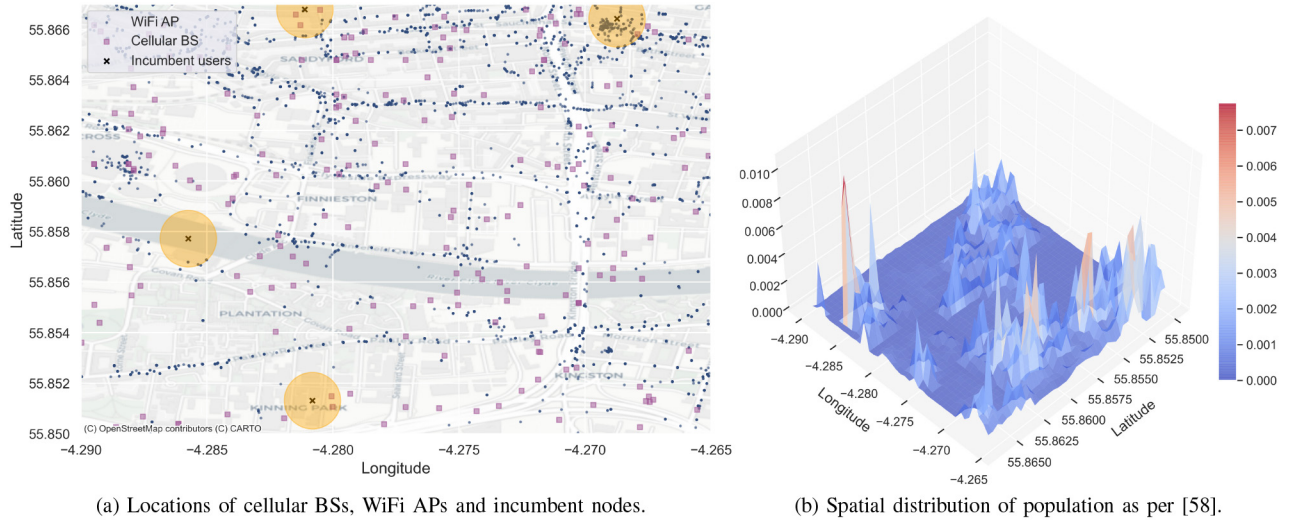


Fig. 14. Real world spatial distribution of network elements and users over the map of Glasgow, U.K.

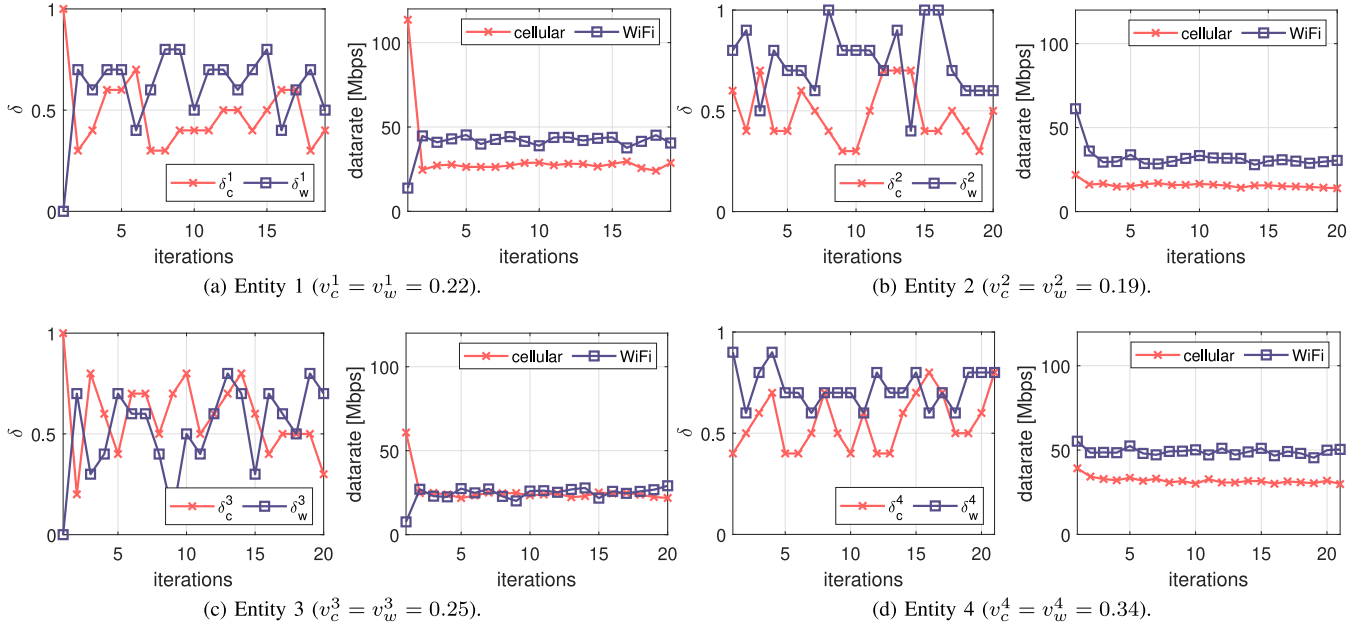


Fig. 15. Interaction of four entities in the city of Glasgow. Parameters: $\theta_c = 5\theta_w$.

of the cellular and WiFi networks interact such that the minimum datarate requirement of each entity is met at equilibrium.

In Fig. 13, the cellular and WiFi datarate thresholds are crossed by each entity. It must be noted that the entities have their WiFi datarate inversely proportional to the WiFi network share. We calculate Jain's fairness index [54] and find that the fairness index for cellular users is 1 whereas for the WiFi users it is 0.9973, and for all the users it is 0.8828. A higher fairness index indicates that the data rates of the users are comparable and close to each other in numerical value.

VI. CASE STUDY: GLASGOW, U.K.

In this section we test our framework on real-world network of Glasgow, U.K. spanning 55.85°N to 55.867°N in latitude and 4.265°W to 4.29°W in longitude. The choice of Glasgow is motivated by the availability of WiFi network data [55]

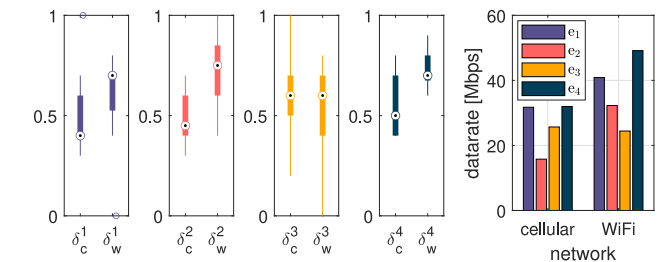


Fig. 16. Box plot of action vector values of each entity and the resultant average datarate achieved by them.

published by the Glasgow City Council. The data for cell tower locations is downloaded from Open Cell ID [56]. However, to determine the positions of the incumbent nodes, we relied on manual data extraction based on the readings of FCC

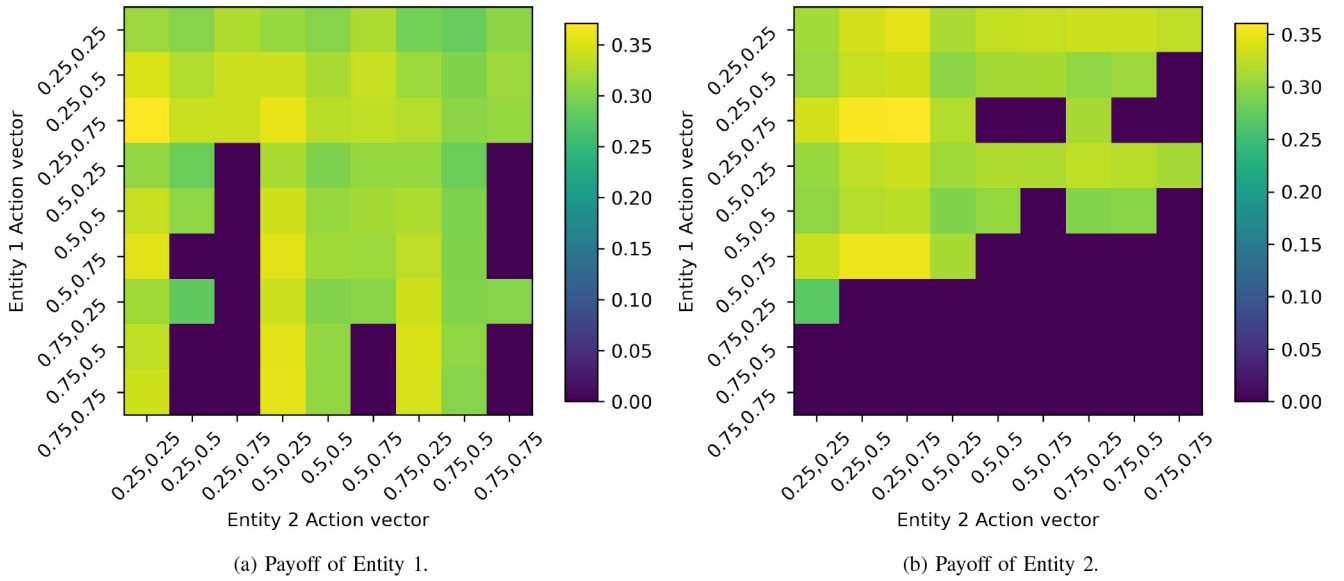


Fig. 17. Normal form representation of the payoffs of two entities, where $\delta_k^i \in \{\frac{1}{4}, \frac{1}{2}, \frac{3}{4}\}$, $k \in \{c, w\}$, $i \in \{1, 2\}$.

documents [1], [2]. We partition the set of all network elements (cellular and WiFi) among multiple entities based on the market shares⁵ of different Telecommunication operators in U.K. [57, Table 36]. The case study captures the behavior of D-BRA when the spatial distribution of the users, APs and BSs are non uniform (see Fig. 14).

The network elements of each entity monitor the QoS delivered to its users through crowdsourcing. This way, the entities are able to evaluate the average QoS performance, and use that to compute the utility in the algorithm.

In Fig. 15, we show how the four entities adjust their action vectors to maximize their own utility. The action vectors do not stabilize, however the average datarate delivered by the cellular and WiFi networks of each entity become saturated. The results hint at the existence of a mixed strategy Nash equilibrium, which we can see if we let the game continue for a sufficiently large number of iterations. In Fig. 16, we convey through box plots, the characteristics of the action vectors of each entity, and show a comparative bar plot of the average datarates achieved by them as a result of playing the game.

VII. CONCLUSION

In this work, we provided a game-theoretic framework for analyzing the interaction between different networks, namely, cellular, WiFi or a combination of both, as they utilize the unlicensed spectrum in addition to their licensed spectra, in the presence of incumbent nodes. We have shown how the system parameters affect the performance of a network at equilibrium and quantified the performance gains of the networks as a result of using the 6 GHz bands, which offer larger bandwidths. The proposed distributed algorithm outperforms the random-strategic baseline and gives an average datarate boost of $\sim 11\%$ and $\sim 18\%$ for cellular and WiFi networks respectively.

⁵EE: 22%, O2: 19%, Vodafone + Three: 25%, others: 34%.

The proposed framework is flexible and can be used to model a variety of scenarios for feasibility and performance assessment of the networks involved. For example, we can analyze how the deployment densities of the WiFi and cellular networks affect the equilibrium. In the absence of incumbent nodes, the framework reduces to multi-entity spectrum sharing. Moreover, the utility maximization problem can be solved using online learning algorithms [59] instead of exhaustive search for a near optimal yet agile performance. The theoretical analysis was done in a stochastic setup and we focused on a large-scale network. Lastly, we tested our framework on a real world location with real cellular network and WiFi AP deployments and showed that a practical implementation of multi-entity spectrum sharing is feasible.

APPENDIX

A. Laplace Transforms

The Laplace transform of the interference [40] experienced by the cellular users in the unlicensed band from transmitters of type $j \in \{c, w, z\}$ is mathematically expressed as $\mathcal{L}_{c,j|U}(s)$:

$$\mathcal{L}_{c,j|U}(s) \stackrel{j \neq c}{=} \exp\left(-\pi\lambda_j|U \frac{(s p_j)^{\frac{2}{\alpha}}}{\text{sinc}\left(\frac{2}{\alpha}\right)}\right),$$

$$\stackrel{j = c}{=} \exp\left(-\int_r^\infty \frac{2\pi\lambda_c|U}{1 + (s p_c)^{-1} x^\alpha} x dx\right).$$

Similarly, the Laplace transform of the interference experienced by the WiFi users in the unlicensed band from the transmitters of type $j \in \{c, w, z\}$ is mathematically expressed as $\mathcal{L}_{w,j|U}(s)$:

$$\mathcal{L}_{w,j|U}(s) = \exp\left(-\pi\lambda_j|U \frac{(s p_j)^{\frac{2}{\alpha}}}{\text{sinc}\left(\frac{2}{\alpha}\right)}\right).$$

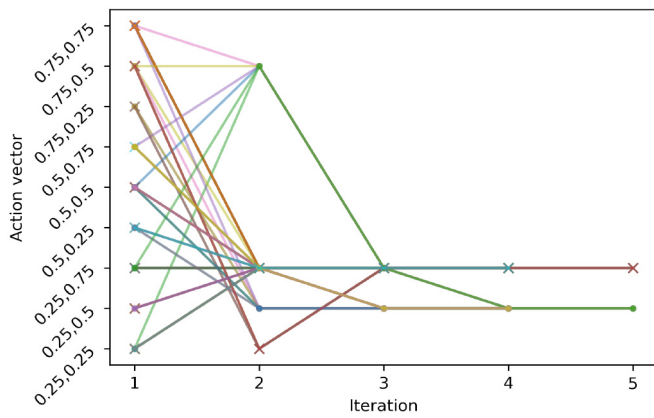


Fig. 18. Temporal evolution of action vector of entity 1 (·) and entity 2 (×).

B. Normal Form Game

In a two-entity interaction, we discretize the action space into $\{\frac{1}{4}, \frac{1}{2}, \frac{3}{4}\} \times \{\frac{1}{4}, \frac{1}{2}, \frac{3}{4}\}$, which allows us to represent the game in normal form (see Fig. 17). Then we find the Nash Equilibrium using the Python library `Nashpy` [60]. We also find the Nash equilibrium through D-BRA by initializing the action vector randomly. In all cases, we converge to the same solution (see Fig. 18), as obtained through `Nashpy`, i.e., $[(\frac{1}{4}, \frac{1}{2}), (\frac{1}{4}, \frac{3}{4})]$.

REFERENCES

- [1] "Report and order and further notice of proposed rulemaking: in the matter of unlicensed use of the 6 GHz band," Federal Commun. Commission, Washington, DC, USA, document ET Docket 18-295, Apr. 2020. [Online]. Available: <https://docs.fcc.gov/public/attachments/FCC-20-51A1.pdf>
- [2] "Expanding flexible use in mid-band spectrum between 3.7 and 24 GHz," Federal Commun. Commission, Washington, DC, USA, document GN Docket 17-183, Apr. 2020. [Online]. Available: <https://docs.fcc.gov/public/attachments/FCC-20-51A1.pdf>
- [3] "Notice of Ofcom's changes to licence exemption for wireless telegraphy devices and consultation on licensing equipment in 57 to 71 GHz," Office Commun., London, U.K., Rep., Jan. 2021. [Online]. Available: https://www.ofcom.org.uk/_data/assets/pdf_file/0030/208857/licence-exemption-notice-2020-condoc.pdf
- [4] Broadcom. "Saudi Arabia's historic designation further drives worldwide momentum for Wi-Fi 6E." Broadcom Blogs, Mar. 2021. [Online]. Available: <https://www.broadcom.com/blog/historic-designation-for-saudi-arabia-further-worldwide-momentum-for-Wi-Fi-6e/>
- [5] M. Warburton. "Canada opens 6GHz band for Wi-Fi, tripling spectrum access." Reuters, May 2021. [Online]. Available: <https://www.reuters.com/technology/canada-opens-6GHz-band-Wi-Fi-tripling-spectrum-access-2021-05-19/>
- [6] "Technical specification group radio access network; study on NR-based access to unlicensed spectrum (release 16)," 3rd Gener. Partnership Project, Sophia Antipolis, France, Rep. (TR) 38.889, Dec. 2018.
- [7] "Feasibility study on 6 GHz for LTE and NR in licensed and unlicensed operations (release 16)," 3rd Gener. Partnership Project, Sophia Antipolis, France, Rep. (TR) 37.890, Dec. 2019.
- [8] V. Sathya, S. M. Kala, M. I. Rochman, M. Ghosh, and S. Roy, "Standardization advances for cellular and Wi-Fi coexistence in the unlicensed 5 and 6 GHz bands," *GetMobile Mobile Comput. Commun.*, vol. 24, no. 1, pp. 5–15, 2020.
- [9] "Deploying 6 GHz RLANs while protecting the fixed service. comments to the FCC GN docket no. 17-183," Fixed Wireless Commun. Coalition, Washington, DC, USA, Rep., Jul. 2019. [Online]. Available: <https://bit.ly/3odu4b3>
- [10] "Propagation models and interference protection criteria for sharing between the fixed service and unlicensed devices in the 6GHz band, version V1.0.0," Wireless Innov. Forum, Reston, VA, USA, Rep. WINNF-TR-1002, Dec. 2019.
- [11] G. Naik, J.-M. Park, J. Ashdown, and W. Lehr, "Next generation Wi-Fi and 5G NR-U in the 6 GHz bands: Opportunities and challenges," *IEEE Access*, vol. 8, pp. 153027–153056, 2020.
- [12] E. J. Oughton, W. Lehr, K. Katsaros, I. Selinis, D. Bubley, and J. Kusuma, "Revisiting wireless Internet connectivity: 5G vs Wi-Fi 6," *Telecommun. Policy*, vol. 45, no. 5, 2021, Art. no. 102127.
- [13] "Joint NGMN/WBA RAN convergence paper," WBA NGMN Alliance, Frankfurt am Main, Germany, Rep. 1, Aug. 2019. [Online]. Available: <https://www.ngmn.org/publications/joint-ngmn-wba-ran-convergence-paper.html>
- [14] A. Chaoub et al., "6G for bridging the digital divide: Wireless connectivity to remote areas," 2020, *arXiv:2009.04175*.
- [15] L. Montsi, L. Mfupe, F. Mekuria, and D. Macleod, "A real-time big-data system for smart spectrum sharing: Enabling affordable broadband in 5G for underserved communities," in *Proc. Global Wireless Summit (GWS)*, 2017, pp. 245–251.
- [16] A. V. Kini, L. Canonno-Velasquez, M. Hosseinian, M. Rudolf, and J. Stern-Berkowitz, "Wi-Fi-LAA coexistence: Design and evaluation of listen before talk for LAA," in *Proc. Annu. Conf. Inf. Sci. Syst. (CISS)*, 2016, pp. 157–162.
- [17] E. J. S. Cabrera, L. Guijarro, and P. Maillé, "Game theoretical analysis of a multi-MNO MVNO business model in 5G networks," *Electronics*, vol. 9, no. 6, p. 933, 2020.
- [18] G. Naik, J. Liu, and J.-M. J. Park, "Coexistence of wireless technologies in the 5 GHz bands: A survey of existing solutions and a roadmap for future research," *IEEE Commun. Surveys Tuts.*, vol. 20, no. 3, pp. 1777–1798, 3rd Quart., 2018.
- [19] C. Cano and D. J. Leith, "Unlicensed LTE/WiFi coexistence: Is LBT inherently fairer than CSAT?" in *Proc. IEEE Int. Conf. Commun. (ICC)*, 2016, pp. 1–6.
- [20] M. Mehrnosh, S. Roy, V. Sathya, and M. Ghosh, "On the fairness of Wi-Fi and LTE-LAA coexistence," *IEEE Trans. Cogn. Commun. Netw.*, vol. 4, no. 4, pp. 735–748, Dec. 2018.
- [21] S. Lagen et al., "New radio beam-based access to unlicensed spectrum: Design challenges and solutions," *IEEE Commun. Surveys Tuts.*, vol. 22, no. 1, pp. 8–37, 1st Quart., 2019.
- [22] P. Wang, B. Di, and L. Song, "Unlicensed spectrum sharing with WiGig in millimeter-wave cellular networks in 6G era," in *Proc. IEEE Global Commun. Conf. (GLOBECOM)*, 2020, pp. 1–6.
- [23] H. Bao, Y. Huo, X. Dong, and C. Huang, "Joint time and power allocation for 5G NR unlicensed systems," *IEEE Trans. Wireless Commun.*, vol. 20, no. 9, pp. 6195–6209, Sep. 2021.
- [24] P. C. Pinto, A. Giorgetti, M. Z. Win, and M. Chiani, "A stochastic geometry approach to coexistence in heterogeneous wireless networks," *IEEE J. Sel. Areas Commun.*, vol. 27, no. 7, pp. 1268–1282, Sep. 2009.
- [25] A. Bhorkar, C. Ibars, and P. Zong, "Performance analysis of LTE and Wi-Fi in unlicensed band using stochastic geometry," in *Proc. IEEE 25th Annu. Int. Symp. Pers. Indoor Mobile Radio Commun. (PIMRC)*, 2014, pp. 1310–1314.
- [26] G. Naik and J.-M. J. Park, "Coexistence of Wi-Fi 6E and 5G NR-U: Can we do better in the 6 GHz bands?" in *Proc. IEEE INFOCOM Conf. Comput. Commun.*, 2021, pp. 1–10.
- [27] A. M. Voicu, L. Simić, and M. Petrova, "Inter-technology coexistence in a spectrum commons: A case study of Wi-Fi and LTE in the 5-GHz unlicensed band," *IEEE J. Sel. Areas Commun.*, vol. 34, no. 11, pp. 3062–3077, Nov. 2016.
- [28] Y. Wu, B. Wang, K. J. R. Liu, and T. C. Clancy, "Repeated open spectrum sharing game with cheat-proof strategies," *IEEE Trans. Wireless Commun.*, vol. 8, no. 4, pp. 1922–1933, Apr. 2009.
- [29] B. Wang, Y. Wu, Z. Ji, K. J. R. Liu, and T. C. Clancy, "Game theoretical mechanism design methods," *IEEE Signal Process. Mag.*, vol. 25, no. 6, pp. 74–84, Nov. 2008.
- [30] F. Teng, D. Guo, and M. L. Honig, "Sharing of unlicensed spectrum by strategic operators," *IEEE J. Sel. Areas Commun.*, vol. 35, no. 3, pp. 668–679, Mar. 2017.
- [31] C. Hasan, M. K. Marina, and U. Challita, "On LTE-WiFi coexistence and inter-operator spectrum sharing in unlicensed bands: Altruism, cooperation and fairness," in *Proc. 17th ACM Int. Symp. Mobile Ad Hoc Netw. Comput.*, 2016, pp. 111–120.
- [32] L. Sboui, Z. Rezki, and M.-S. Alouini, "Achievable rate of spectrum sharing cognitive radio systems over fading channels at low-power regime," *IEEE Trans. Wireless Commun.*, vol. 13, no. 11, pp. 6461–6473, Nov. 2014.
- [33] A. K. Bairagi, S. F. Abedin, N. H. Tran, D. Niyato, and C. S. Hong, "QoE-enabled unlicensed spectrum sharing in 5G: A game-theoretic approach," *IEEE Access*, vol. 6, pp. 50538–50554, 2018.

- [34] X. Chen, X. Gong, L. Yang, and J. Zhang, "A social group utility maximization framework with applications in database assisted spectrum access," in *Proc. IEEE INFOCOM Conf. Comput. Commun.*, 2014, pp. 1959–1967.
- [35] A. K. Bairagi, N. H. Tran, W. Saad, Z. Han, and C. S. Hong, "A game-theoretic approach for fair coexistence between LTE-U and Wi-Fi systems," *IEEE Trans. Veh. Technol.*, vol. 68, no. 1, pp. 442–455, Jan. 2019.
- [36] K. Hamidouche, W. Saad, M. Debbah, M. T. Thai, and Z. Han, "Contract-based incentive mechanism for LTE over unlicensed channels," *IEEE Trans. Commun.*, vol. 67, no. 9, pp. 6427–6440, Sep. 2019.
- [37] A. U. Rahman, M. A. Kishk, and M.-S. Alouini, "Coexistence at unlicensed bands." Github. Sep. 2021. [Online]. Available: <https://github.com/Aniq55/coexistence>
- [38] M. A. Kishk and H. S. Dhillon, "Tight lower bounds on the contact distance distribution in Poisson hole process," *IEEE Wireless Commun. Lett.*, vol. 6, no. 4, pp. 454–457, Aug. 2017.
- [39] M. A. Kishk and H. S. Dhillon, "Coexistence of RF-powered IoT and a primary wireless network with secrecy guard zones," *IEEE Trans. Wireless Commun.*, vol. 17, no. 3, pp. 1460–1473, Mar. 2018.
- [40] A. M. Hayajneh, S. A. R. Zaidi, D. C. McLernon, M. Di Renzo, and M. Ghogho, "Performance analysis of UAV enabled disaster recovery networks: A stochastic geometric framework based on cluster processes," *IEEE Access*, vol. 6, pp. 26215–26230, 2018.
- [41] "Google Fi." Google. 2021. [Online]. Available: <https://fi.google.com/>
- [42] B. Blaszczyzyn, M. Haenggi, P. Keeler, and S. Mukherjee, *Stochastic Geometry Analysis of Cellular Networks*. Cambridge, U.K.: Cambridge Univ. Press, 2018.
- [43] S. Durand, F. Garin, and B. Gaujal, "Distributed best response algorithms for potential games," in *Proc. Eur. Control Conf. (ECC)*, 2018, pp. 2170–2175.
- [44] D. Fudenberg, F. Drew, D. K. Levine, and D. K. Levine, *The Theory of Learning in Games*, vol. 2. Cambridge, MA, USA: MIT Press, 1998.
- [45] J. W. Friedman, "A non-cooperative equilibrium for supergames," *Rev. Econ. Stud.*, vol. 38, no. 1, pp. 1–12, 1971.
- [46] G.-H. Demeze-Jouatsa, "A complete folk theorem for finitely repeated games," *Int. J. Game Theory*, vol. 49, no. 4, pp. 1129–1142, 2020.
- [47] R. D. Luce and H. Raiffa, *Games and Decisions: Introduction and Critical Survey*. New York, NY, USA: Courier Corp., 1989.
- [48] M. J. Osborne and A. Rubinstein, *A Course in Game Theory*. Cambridge, MA, USA: MIT Press, 1994.
- [49] NR: *User Equipment (UE) Radio Transmission and Reception; Part 1: Range 1 Standalone, Release 16.4.0*, 3GPP Standard (TS) 38.101-1, Jul. 2020. [Online]. Available: <https://www.3gpp.org/DynaReport/38101-1.htm>
- [50] D. López-Pérez, A. Garcia-Rodríguez, L. Galati-Giordano, M. Kasslin, and K. Doppler, "IEEE 802.11be extremely high throughput: The next generation of Wi-Fi technology beyond 802.11ax," *IEEE Commun. Mag.*, vol. 57, no. 9, pp. 113–119, Sep. 2019.
- [51] ITU, *Handbook on Land Mobile* (Including Wireless Access), vol. 1, 2nd ed. Geneva, Switzerland: Int. Telecommun. Union, 2001. [Online]. Available: <https://www.itu.int/pub/R-HDB-25>
- [52] A. Weissberger, "5G base station deployments; open-RAN competition & huge 5G BS power problem." Comsoc Techblog. Aug. 2020. [Online]. Available: <https://techblog.comsoc.org/2020/08/07/5G-base-station-deployments-open-ran-competition-huge-5G-bs-power-problem/>
- [53] M. Ding, D. Lopez-Perez, H. Claussen, and M. A. Kaafar, "On the fundamental characteristics of ultra-dense small cell networks," *IEEE Netw.*, vol. 32, no. 3, pp. 92–100, May/June. 2018.
- [54] K. Jones and L. Liu, "What where Wi: An analysis of millions of Wi-Fi access points," in *Proc. IEEE Int. Conf. Portable Inf. Devices*, 2007, pp. 1–4.
- [55] C. Sun and R. Jiao, "Discrete exclusion zone for dynamic spectrum access wireless networks," *IEEE Access*, vol. 8, pp. 49551–49561, 2020.
- [56] R. Jain, A. Durrresi, and G. Babic, "Throughput fairness index: An explanation," ATM Forum Contribution, Washington, DC, USA, document ATM_Forum/99-0045, 1999.
- [57] "Wi-Fi access point locations." Glasgow City Council. Feb. 2014. [Online]. Available: <http://ubdc.gla.ac.uk/nl/dataset/Wi-%20Acce%20Poi%20Locations>
- [58] "Cell tower data. License: CC-BY-SA 4.0." Open Cell ID. Sep. 2021. [Online]. Available: <https://my.opencellid.org/>
- [59] "Ofcom technology tracker—H1." Ofcom. 2021. [Online]. Available: https://www.ofcom.org.uk/_data/assets/pdf_file/0015/219102/technology-tracker-2021-data-tables.pdf
- [60] Facebook. "High resolution population density maps." Humanitarian Data Exchange (HDX). Sep. 2021. [Online]. Available: <https://dataforgood.facebook.com/dfg/tools/high-resolution-population-density-maps>
- [61] A. U. Rahman, G. Ghatak, and A. De Domenico, "An online algorithm for computation offloading in non-stationary environments," *IEEE Commun. Lett.*, vol. 24, no. 10, pp. 2167–2171, Oct. 2020.
- [62] V. Knight and J. Campbell, "Nashpy: A python library for the computation of nash equilibria," *J. Open Sour. Softw.*, vol. 3, no. 30, p. 904, 2018.



Forum in Heidelberg, Germany.

Aniq Ur Rahman received the bachelor's degree in electronics and communication engineering from the National Institute of Technology Durgapur, India, in 2019, and the master's degree in electrical and computer engineering from the King Abdullah University of Science and Technology, Saudi Arabia, in 2022. He is currently pursuing the D.Phil. degree in engineering science with the Information and Network Science Lab, University of Oxford, U.K. He was selected among 200 young researchers worldwide to attend the 7th Heidelberg Laureate



Mustafa A. Kishk (Member, IEEE) received the B.Sc. and M.Sc. degrees in electrical engineering from Cairo University in 2013 and 2015, respectively and the Ph.D. degree in electrical engineering from Virginia Tech in 2018. He is an Assistant Professor with Maynooth University, Ireland. From 2019 to 2022 he was a Postdoctoral Research Fellow with the King Abdullah University of Science and Technology. His research interests include UAV communications, satellite communications, and global connectivity for rural and remote areas.



performance analysis of wireless communication systems.

Mohamed-Slim Alouini (Fellow, IEEE) was born in Tunis, Tunisia. He received the Ph.D. degree in electrical engineering from the California Institute of Technology, Pasadena, CA, USA, in 1998. He served as a Faculty Member with the University of Minnesota, USA, then with the Texas A&M University at Qatar, Qatar, before joining King Abdullah University of Science and Technology, Saudi Arabia, as a Professor of Electrical Engineering in 2009. His current research interests include the modeling, design, and